Treatment-Specific Composition of Gut Microbiota Is Associated with Disease Remission in a Pediatric Crohn's Disease Cohort

Running Title: Microbiota and Pediatric Crohn's Disease Remission

Daniel Sprockett, MSc[1*], Natalie Fischer, PhD[2*], Rotem Sigall Boneh, RD[3], Dan Turner, MD[4], Jarek Kierkus, MD, PhD[5], Malgorzata Sladek, MD, PhD[6], Johanna C. Escher, MD, PhD[7], Eytan Wine, MD, PhD[8], Baruch Yerushalmi, MD[9], Jorge Amil Dias, MD[10], Ron Shaoul, MD[11], Michal Kori, MD[12], Scott B. Snapper, MD, PhD[13,14], Susan Holmes, PhD[15], Athos Bousvaros, MD[13], Arie Levine, MD[3,16†], and David A. Relman, MD[1,2,17†]

1. Department of Microbiology & Immunology, Stanford University School of Medicine, Stanford, CA 94305, USA
2. Division of Infectious Diseases & Geographic Medicine, Department of Medicine, Stanford University School of Medicine, Stanford, CA 94305, USA
3. Pediatric Gastroenterology and Nutrition Unit, Wolfson Medical Center, Holon, Israel
4. The Juliet Keidan Institute of Pediatric Gastroenterology & Nutrition, Shaare Zedek Medical Center, The Hebrew University of Jerusalem, Jerusalem, Israel
5. Department of Gastroenterology, Hepatology, Feeding Disorders and Pediatrics, The Children's Memorial Health Institute, Warsaw, Poland
6. Department of Pediatrics, Gastroenterology and Nutrition, Jagiellonian University Medical College, Cracow, Poland
7. Department of Pediatric Gastroenterology, Erasmus MC-Sophia Children's Hospital, Rotterdam, The Netherlands
8. Division of Pediatric Gastroenterology and Nutrition, Department of Pediatrics, University of Alberta, Edmonton, Canada

9. Pediatric Gastroenterology Unit, Soroka University Medical Center, and Faculty of Health Sciences, Ben-Gurion University of the Negev, Beer Sheva, Israel

10. Department of Pediatrics, Hospital de Sao Joao, Porto, Portugal

11. Pediatric Gastroenterology Unit, Ruth Children's Hospital, Rambam Medical Center, Haifa, Israel

12. Pediatric Day Care Unit, Kaplan Medical Center, Rehovot, Israel

13. Division of Gastroenterology, Hepatology, and Nutrition, Boston Children's Hospital, Boston, MA 02115, USA

14. Division of Gastroenterology, Brigham and Women's Hospital, and Harvard Medical School, Boston, MA, 02115, USA

15. Department of Statistics, Stanford University, Stanford, CA 94305, USA

16. Sackler School of Medicine, Tel Aviv University, Tel Aviv, Israel

17. Infectious Diseases Section, Veterans Affairs Palo Alto Health Care System, Palo Alto, CA 94304, USA

* These authors contributed equally to this work.

† These authors contributed equally to this work.

Correspondence: D.A.R. (email: relman@stanford.edu)

Study Highlights:

What is known:

- The composition of the intestinal microbiota of pediatric Crohn's disease patients is altered, and has low diversity
- Antibiotics disturb the intestinal microbiota in an individualized fashion that may help explain different clinical responses
- The combination of metronidazole and azithromycin (MET+AZ) is more effective than metronidazole alone (MET) for inducing disease remission in some CD patients

What is new:

- MET and MET+AZ cause distinct changes in the gut microbiota of pediatric CD patients
- Each regimen induces a specific remission-associated microbiota community configuration
- Disease remission after either antibiotic regimen is characterized by a higher abundance of *Lactobacillus*

Abstract (226 words; max permitted = 250)

Objectives: The beneficial effects of antibiotics depend in part on the gut microbiota but are inadequately understood. We investigated the impact of metronidazole (MET) and metronidazole plus azithromycin (MET+AZ) on the microbiota in pediatric CD, and the use of microbiota features as classifiers or predictors of disease remission.

Methods: 16S rRNA-based microbiota profiling was performed on stool samples from a multinational, randomized, controlled, longitudinal, 12-week trial of MET vs. MET+AZ in children with mild to moderate CD. Profiles were analyzed together with disease activity, and then used to construct Random Forest classification models to classify remission or predict treatment response.

Results: Both MET and MET+AZ significantly decreased diversity of the microbiota and caused large treatment-specific shifts in microbiota structure at week 4. Disease remission was associated with a treatment-specific microbiota configuration. Random Forest models constructed from microbiota profiles pre- and during antibiotic treatment with metronidazole accurately classified disease remission in this treatment group (AUC of 0.879, 95% CI 0.683, 0.9877; sensitivity 0.7778; specificity 1.000, $P < 0.001$). A Random Forest model trained on pre-antibiotic microbiota profiles predicted disease remission at week 4 with modest accuracy (AUC of 0.8, $P = 0.24$).

Conclusions: MET and MET+AZ antibiotic regimens lead to distinct gut microbiota structures at remission. It may be possible to classify and predict remission based in part on microbiota profiles, but larger cohorts will be needed to realize this goal.

Keywords: pediatric Crohn's disease; microbiota; antibiotics; metronidazole; azithromycin; disease remission; 16S rRNA gene; Random Forest models

INTRODUCTION

The global incidence of Crohn's disease (CD) has steadily risen over the past few decades, especially among pediatric patients (1). Large efforts are being made to identifying novel non-invasive biomarkers not only to monitor disease severity but also to predict therapeutic response in CD patients (2,3).

Genome-wide association studies have identified a variety of risk loci within genes important for the maintenance of homeostasis with our commensal gut microbiota (4). In this regard, several studies in pediatric CD patients have described a state of microbiome 'dysbiosis', with varying claims about disease-promoting or -ameliorating bacterial taxa (5-7) and about differences in bacterial diversity (8). Previous work showed that the magnitude of antibiotic effects on the microbiota differs among individuals, and that some taxa show interindividual variation in the response to a single antibiotic treatment (9). Similarly, several trials in adult CD found, in general, a benefit of antibiotic treatment, but with very heterogeneous results for the use of metronidazole, quinolones, and rifaximin (10).

The goal of this study was to evaluate the impact of metronidazole (MET) and the combination of metronidazole and azithromycin (MET+AZ) on the intestinal microbiota of pediatric CD patients. We show that both antibiotic regimens led to a decrease in gut microbiota diversity, but also exerted a treatment-specific impact on the microbiota. Of note, we show that these two antibiotic regimens produced distinct alterations in microbiota structure associated with disease remission. We used machine-learning techniques to identify microbiota composition-based signatures associated with antibiotic treatment that might enable monitoring of disease and guide clinical decision making.

METHODS

Study Design

Seventy-four CD patients (age 5–18 years) were enrolled at 11 pediatric gastroenterology clinical sites in an investigator-blinded randomized controlled trial comparing the efficacy of MET+AZ versus MET therapy for the treatment of children with mild to moderate active CD (10 < Pediatric Crohn's Disease Activity Index (PCDAI) ≤ 40) (National Institutes of Health NCT01596894). A complete description of the study design, laboratory and analysis methods, and primary outcomes was published previously (11). The treatment protocol was adapted from a report by Levine and Turner (12). Patients were enrolled in one of the two treatment arms with 1:1 randomization, although 11 subjects with lack of response to MET therapy received open-label azithromycin between weeks 4 and 8. These MET/MET+AZ subjects were treated as a separate group for analyses involving time points after week 4. Furthermore, 4 patients in the MET group, 5 patients in the MET+AZ group and 1 patient in the MET/MET+AZ group received steroids or biologics after week 4 at their physician's direction due to inadequate response. Both MET and MET+AZ groups discontinued antibiotics after week 8, while the MET/MET+AZ group maintained their regimen to complete a total of 8 weeks. Disease activity was determined at weeks 0, 4, 8 and 12 using the PCDAI, when stool samples were collected for microbiota analysis. Clinical remission was defined as PCDAI < 10. All patients provided written informed consent, or assent when required, prior to participation. The study was conducted according to the principles of the Declaration of Helsinki.

Microbiota Analysis

Stool samples were collected and frozen on site at -20°C and then shipped to a central laboratory and stored at -80°C until further processing. DNA was extracted from ~200 mg stool using the QIAGEN DNeasy PowerSoil HTP 96 Kit (Cat #12955-4) following the manufacturer's instructions, including a 2 x 10 minute bead-beating step using the Retsch 96 Well Plate Shaker at speed 20. The V4 region of the 16S rRNA gene was amplified using forward primer 515F (5′-

GTGCCAGCAGCCGCGGTAA-3′) with an error-correcting barcode and 806R (5′-GGACTACCAGGGTATCTAAT-3′) (13). PCR products were then purified, pooled in equimolar concentrations, and sequenced on three 2 x 300 Illumina MiSeq paired-end runs using reagent kit v3.

Raw reads were demultiplexed using the QIIME command `split_libraries_fastq.py` (QIIME version 1.9.1) and then quality trimmed using the DADA2 pipeline (`dada2` version 1.1.1) in R (R version 3.2.4) (14). Briefly, forward reads were truncated to 220 bp, and reverse reads to 150 bp, and quality filtered with settings `maxN=0, maxEE=2, truncQ=2`. Following quality trimming, amplicon sequence variants (ASVs) were inferred using the DADA2 pipeline. Taxonomy was assigned to each ASV using the RDP classifier and the SILVA 16S rRNA database (SILVA nr version 132), and a phylogenetic tree was built from the ASVs using the `phangorn` R package (`phangorn` version 2.4.0). The ASV table, patient sample data, taxonomy assignments, phylogenetic tree, and ASV sequences were then bundled into a single `phyloseq` data object for further plotting and statistical analysis (`phyloseq` version 1.24.2) (15).

Faith's Phylogenetic Diversity was calculated using the R package `picante` (`picante` version 1.7), and distance calculations and ordination plots were built using the `phyloseq` package. Hierarchical clustering of ASVs was performed using the `hclust` function in the `stats` R package (`stats` version 3.5.1). Differential abundance tests were carried out using the `DESeq2` R package (`DESeq2` version 1.20.0).

Random Forest Modeling

Machine learning analyses were performed using the `caret` and `randomForest` R packages (`caret` version 6.0.80, `randomForest` version 4.6.14). Prior to model building, the ASV

abundance was transformed using a variance stabilizing transformation to normalize for sequencing depth in the `DESeq2` R package, as well as centered to reduce the influence of inter-individual variation. Models were constructed on microbiota data from either weeks 4 and 8 (Model 1), or weeks 0, 4 and 8 (Model 2) from subjects in the MET group, with the outcome variable being disease state (i.e., remission or non-remission) at the time of sample collection. Each model was trained on samples from a random subset of 70% of subjects, with 1000 trees and leave-one-out cross-validation. To assess their accuracy, models were used to predict remission or non-remission on samples from the remaining 30% of subjects. Both sets of classification results were then evaluated by calculating their area under the curve (AUC), as derived from a receiver operating characteristic (ROC) curve analysis using the R package `ROCR` (`ROCR` version 1.0.7). Each model also calculated importance scores for ASVs based on the increase in prediction error when the ASV in question was left out of the training set via random permutation.

A Random Forest model was constructed on all pre-antibiotic (week 0) microbiota data, as well as on clinical data, including sex, age, disease duration, tissue involvement (Paris classification), baseline immunomodulators, baseline CRP and PCDAI to predict disease state (remission or non-remission) at week 4 in both treatment groups combined. In order to increase the number of shared features found across samples and decrease the noise among closely-related bacterial taxa, ASVs were agglomerated based on their cophenetic distance in the phylogenetic tree at the `h = 0.3` level. These numbered ASV clusters were also labeled by the number of ASVs in the cluster, as well as the genus that was assigned to the majority of the ASVs within the cluster. If >50% of the ASVs within a cluster were not assigned to a single genus, the same majority rule was used iteratively at higher taxonomic levels. Models were constructed and tested as described above. Abundance was normalized using variance stabilizing transformation (vst).

Amplicon sequencing data are available at SRA (project ID pending). A detailed description of this analysis, along with all analysis code and raw data used to go from sequences to final figures, is available at the Stanford Digital Repository (purl.stanford.edu/XXX) and as Supplementary Material.

RESULTS

Clinical Outcomes

A total of 67 subjects from 9 sites provided stool samples for microbiome analysis and are included in the present study (Table 1). Of this group, 36 children were randomly assigned to receive MET, and 31 received MET+AZ (Fig. 1a). Fig. 1b shows the temporal dynamics of each patient's PCDAI at the time of stool sample collection (Fig. 1b). By week 4, 42% (15/36) of MET subjects and 65% (20/31) of MET+AZ subjects had achieved remission (Fig. 1b). Between weeks 4 and 8, 11 of the MET subjects failing remission had azithromycin added to their treatment regimen (MET/MET+AZ). At week 8, 60% (15/25) patients in the remaining MET group, 65% (20/31) in the MET+AZ group, and 45% (5/11) in the new MET/MET+AZ group had achieved remission. Of note, 4 patients in the MET group and 5 patients in the MET+AZ group who did not respond to antibiotic treatment by week 4 received open-label steroids or biologics. Therefore, not all improvement in disease in these patients could necessarily be attributed to the antibiotic regimen alone. At week 12, 72% (18/25) of the remaining MET group were in remission, while 71% (22/31) of the MET+AZ and 100% (11/11) of the MET/MET+AZ group were in remission, respectively.

Microbiota Response to Single and Combination Antibiotic Therapies

Antibiotics can strongly perturb the distal gut microbiota in an individual-specific manner (16); individualized responses might explain some of the observed heterogeneity in disease progression and dynamics.

We observed a profound shift in gut microbiota diversity and structure following antibiotic administration in most subjects. In the MET and MET+AZ treatment groups, alpha diversity decreased significantly (Wilcoxon test, $P \leq 0.01$) (Fig. 2a). Diversity remained low in both groups at week 8, and rebounded towards its pre-antibiotic level by week 12, after discontinuation of antibiotics. Yet, only the MET group achieved a diversity level that was comparable to its baseline state (MET week 0 vs. 12, Wilcoxon test, $P = 0.16$), while the MET+AZ group's mean diversity remained significantly lower (MET+AZ week 0 vs. 12, Wilcoxon test, $P \leq 0.01$).

Subjects in the MET group who were subsequently given AZ (MET/MET+AZ) after week 4, experienced a non-significant decrease in mean diversity at week 4 (week 0 vs week 4, Wilcoxon test, $P = 0.07$), consistent with this sub-group's initial unresponsiveness to MET. However, after the addition of azithromycin at week 8, mean diversity decreased significantly (week 4 vs 8, Wilcoxon test, $P \leq 0.05$), and became comparable to the level of the MET+AZ group at week 4 (Wilcoxon test, $P = 0.2$). Diversity remained low at week 12 in the MET/MET+AZ group, possibly because many subjects were still completing their 8-week combination antibiotic course at that time.

Next, we examined the magnitude of the change in microbiota structure in response to antibiotics by calculating the median difference in unweighted UniFrac distance between samples from the same patient. While we found no significant difference in mean unweighted UniFrac distance between weeks 0 and 4 across treatment groups, the MET/MET+AZ group

showed a significantly larger shift in community structure than the MET group between weeks 4 and 8, possibly reflecting the addition of azithromycin (Fig. 2b).

We then assessed the contribution of current antibiotic use, treatment group, and remission status to variation in the data using principal coordinates analysis (PCoA) based on unweighted Unifrac distances (17). The use of antibiotics at the time of sample collection was a significant source of variation (Fig. 2c) (PERMANOVA with 1000 permutations, $P < 0.001$), as was specific treatment (Fig. 2d) (PERMANOVA, $P < 0.001$) and remission status (PERMANOVA, $P < 0.01$) (Fig. 2e).

In order to identify groups of bacterial taxa with distinct responses to the different antibiotic regimens, we performed differential abundance testing between samples from weeks 0 and 4. ASVs with significant changes in abundance are summarized in a heat map, showing their relative abundance in each treatment group across all time points (Fig. 3). The top three clusters of the heatmap show ASVs that increased in abundance during the period of treatment and then decreased after antibiotics were withdrawn. While ASVs 7 and 61 (both *Enterococcus*) increased in abundance in both treatment groups, ASV 29 (*Streptococcus*) and ASV 27 (*Klebsiella*) increased in the MET group only. This can be explained by the known sensitivity of streptococci and *Klebsiella* to azithromycin and insensitivity to metronidazole (18).

ASVs 18 and 2 (both *Bifidobacterium*) and ASV 4 (*Escherichia-Shigella*) increased in abundance in the MET group, but decreased in the MET+AZ group. The bottom three clusters of the heatmap include ASVs that decreased in abundance during single and/or combination antibiotic treatment and recovered at least partially after cessation of antibiotic administration (Fig. 3). ASVs 10 (*Bacteroides vulgatus*), 114 (*Lachnospiraceae*), 119 (*Lachnoclostridium*), 130 (*Alistipes*), 3 (*Faecalibacterium prausnitzii*), 34 (*Blautia faecis*), 46 (*Alistipes putredinis*), 55

(*Bacteroides caccae*), 57 (*Bacteroides*), 64 (*Terrisporobacter*), 65 (*Coprococcus*), 74 (*Veillonella*) and 97 (*Dorea formicigenerans*) significantly decreased in abundance in the MET treatment group, while ASVs 103 (*Morganella morganii*), 165 (*Parabacteroides distasonis*), 17 (*Haemophilus*), 22 (*Bacteroides*), 25 (*Faecalibacterium*), 268 (*Sutterella*), 35 (*Erysipelatoclostridium ramosum*), 38 (*Bacteroides uniformis*), 50 (*Lachnospiraceae*) and 86 (*Ruminococcaceae*) decreased significantly in the MET+AZ group.

Microbiota and Crohn's Disease remission

To better understand how antibiotics might influence microbiota structure and remission, we calculated pairwise Bray-Curtis dissimilarity scores for remission samples and compared those to the pair-wise scores for non-remission samples in each treatment group. Week 4 and 8 samples from patients in the MET group who were in remission at that time were significantly more similar to each other than they were to week 4 and 8 samples from patients who were not in remission at the time (Wilcoxon text, $P \leq 0.001$) (Fig. 4a). We observed no significant differences for samples from the MET+AZ group. Furthermore, we found that remission samples from weeks 4 and 8 formed distinct clusters reflecting treatment group (PERMANOVA, $P \leq 0.001$), a pattern that was not observed for non-remission samples (Fig. 4b).

Based on these observations, we sought to identify treatment-specific microbial indicators of CD remission. We used Random Forest modeling to predict whether a patient was in remission based on their microbiota structure at that time. First, we constructed a model based on the abundances of ASVs found in remission and non-remission samples collected during antibiotic treatment (Model 1, weeks 4 and 8). Because the numbers of remission and non-remission samples in the MET+AZ group were too uneven to be able to construct a useful model, we focused on the MET group only. This model classified remission in the MET patients with an AUC of 0.777 (95% CI, 0.3229, 0.8366; sensitivity, 0.8750; specificity, 0.2857; *P*

=0.4006), and classified remission in the MET+AZ group with an AUC of 0.68 (95% CI, 0.4066, 0.6764; sensitivity, 0.3846; specificity, 0.8889; *P* = 0.9909) (Fig. 5a), but did not achieve statistical significance in either case. In order to test an alternative model that incorporated a greater number of non-remission samples, we constructed Model 2 with samples from week 0 as well; these samples represent an alternative non-remission state prior to antibiotic administration, but at the same time, these samples introduce antibiotic treatment as a confounding factor (Model 2, weeks 0, 4 and 8). Model 2 classified remission in MET patients with improved accuracy and an AUC of 0.879 (95% CI: 0.683, 0.9877; sensitivity: 0.7778; specificity: 1.000; *P* < 0.001) and remission in the MET+AZ group with a lower AUC of 0.695 (95% CI: 0.5038, 0.7156; sensitivity: 0.20513; specificity: 0.93878; *P* = 0.1672) (Fig. 5a).

Models 1 and 2 each assigned importance scores to each ASV based on the increase in model prediction error when that feature was randomly permuted while all others were left unchanged. The 10 most important ASVs in each model are displayed in Fig. 5b. The most important ASV for both models was ASV 291 (*Lactobacillus*) (Fig 5b). The ASVs with high importance scores had different abundances in pre-antibiotics, remission, and non-remission samples. Compared to their relative abundances in pre-antibiotic samples, we observed a large increase in ASV 291 (*Lactobacillus*), ASV 60 (*Klebsiella*) and ASVs 2 and 154 (both *Bifidobacterium*), specifically in remission samples (Fig. 5c). In agreement with the results shown in Fig. 3. we observed an increase in abundance of ASVs 7 and 61 (both *Enterococcus*) from the pre-antibiotic state, but no discrepancy between remission and no-remission samples. ASVs that decreased in remission samples, but not in non-remission samples, included ASV 16 (*Fusicatenibacter saccharivorans*) and ASV 24 (*Dorea longicatena*).

Next, we were interested in whether there were microbial signatures present prior to antibiotic administration that would predict remission after treatment. Although not statistically

significant, pre-antibiotic samples from MET subjects who were in remission at week 4 trended towards higher alpha diversity (Supplemental Fig. 1a), a pattern reported in other prediction-focused studies (27,28). Due to the limited number of pre-antibiotic samples available, we combined samples from both treatment groups, and information on each subject's age, sex, disease duration, tissue involvement, and the current disease state. Unfortunately, we still were not able to construct a robust model (AUC = 0.8; 95% CI: 0.4099, 0.8666; sensitivity, 0.8; specificity, 0.5; P = 0.24) (Supplemental Fig. 1b). Furthermore, we identified ASV clusters with higher mean abundance in pre-antibiotic samples of subjects that went on to achieve remission, such as Cluster 8 (*Peptostreptococcaceae*), Cluster 24 (*Alistipes*), Cluster 23 (*Clostridium* sensu stricto) and Cluster 27 (*Parabacteroides*) (Supplemental Fig. 1c). In contrast, for example, ASV Cluster 61 (*Fusobacterium*) was more abundant in pre-antibiotic samples of subjects who did not subsequently achieve remission, in accordance with other studies (7).

Discussion

In this study, we determined the effects of MET-only and combination MET+AZ therapy on the gut microbiota in pediatric CD patients. We demonstrated a treatment-specific effect of both antibiotic regimens on microbiota structure, especially at the time of clinical disease remission. We assessed the utility of microbiota signatures for classifying disease remission as well as the capacity of baseline (pre-antibiotic) microbiota structure to predict future treatment response.

In comparison to previous work, the strength of our study lies in the use of samples from a multinational cohort and from CD patients exclusively. Small cohort size is a common problem and has led to co-evaluation of samples from mixed patient populations with CD and ulcerative colitis, while recent data highlight the differences between those subtypes of IBD with respect to the microbiota (19). Second, many previous studies have characterized the microbiota of patients based on one sample and time point (5,7), while the design of this study afforded an

opportunity to monitor the microbiota before, during, and after treatment, which we believe is critical for identifying microbial signatures related to different clinical outcomes.

It is well established that antibiotic treatment creates an ecosystem-wide disturbance and decreases the overall diversity of the gut microbiome (20). To our knowledge few studies have examined the effects of single versus combination antibiotics on the gut microbiome (21). While we observed a general decrease in diversity in response to antibiotics, our results also showed a distinct impact on microbiota structure and a decrease or increase of specific bacterial ASVs in each treatment group. This highlights the need to understand better the additive, antagonistic, synergistic, and non-linear effects of antibiotic treatments with regards to patient outcome. Despite different effects on the gut microbiota, the two treatments produced remission-compatible microbiota configurations.

Metronidazole is one of the most prescribed antibiotics in the treatment of pediatric CD, but to our knowledge, there has been no in-depth study of the effects of metronidazole treatment on the gut microbiota in humans to date. One study in mice, comparing the impact of metronidazole versus streptomycin on the microbiota and subsequent *C. rodentium*-induced colitis, observed treatment specific effects, not only on microbiota structure, but on gut mucosal immune responses as well (22). In the absence of *C. rodentium* infection, metronidazole was found to decrease goblet cell expression of MUC2, thereby leading to a thinning of the inner mucus layer, which could be detrimental for intestinal homeostasis and promote chronic intestinal inflammation. Although this observation has not been confirmed in humans, it has important implications for the use of MET in IBD patients.

Recent studies reported superior outcomes for MET plus AZ as compared to MET alone (19,20). AZ penetrates multiple intestinal compartments, including the intestinal lumen, biofilms

in the mucus layer, as well as macrophages (23,24), which would allow the targeting of various pathogens implicated in CD, such as adherent and invasive *E. coli* (AIEC) strains (25-27). Also, genera such as *Escherichia* and *Haemophilus* have been associated with CD at disease onset in children (13). Our observations of reduced abundances of ASV 4 (*Escherichia/Shigella*) in the MET+AZ group, and increased abundances in the MET group may reflect specific targeting of this taxon by azithromycin in our cohort. To be able to assess the presence of AIEC specifically, patient biopsies could be used in the future to access the mucosa-adherent or intracellular microbial constituents.

We also observed that some bacterial taxa such as *Enterococcus*, *Streptococcus*, *Klebsiella*, *Bifidobacterium* and *Enterobacteriaceae* increased in abundance during antibiotic treatment. This could be due to creation or expansion of nutritional and/or environmental niches during or after general community disturbance, or could indicate intrinsic or acquired antibiotic resistance. Our finding of increased abundances of *Enterococcus* ASVs in both treatment groups is concerning, as they possess multiple mechanisms for resisting antibiotics; their expansion could predispose patients to invasive infections (28,29).

Another important question is whether the microbiome itself might be used as a therapeutic agent for Crohn's disease, for example by administration of specific beneficial microbes as probiotics (30). Our study identified multiple *Lactobacillus* ASVs that were important for the classification of clinical remission and that significantly increased during remission). *Lactobacillus* species are commonly used as probiotics and several *in vitro* and animal studies suggest that they have properties able to reduce inflammation in Crohn's Disease (31,32). In humans, clinical trials with *Lactobacillus* probiotics in CD patients have so far been unsuccessful (33,34), highlighting the need to understand not only the biology of *Lactobacillus* species but microbial community ecology.

Two recent studies predicted the success of biologics based on pre-treatment microbiota data in adult IBD patients (27,28). We also demonstrated that Random Forest models can be useful for microbiota-based classification and prediction. Our efforts in constructing useful classifiers for disease remission or prediction of treatment response to antibiotics draws attention to the importance and difficulties of obtaining sufficient numbers of samples.

In conclusion, there are several important implications to our findings. Our results suggest that there is no single antibiotic induced remission state, but that each regimen may impact the microbiome in an antibiotic-specific manner leading to remission. We showed that the classification of pediatric CD patients in antibiotic-associated clinical remission based on their microbiota structure is possible, although large sample sizes are required for accurate model construction. We demonstrated that classification and prediction models based on microbiota signatures may be another tool for monitoring disease and treatment response. Moreover, they may also support the development and testing of more precise approaches for microbiome manipulation and could eventually lead to more effective management of CD and other inflammatory bowel disease.

Acknowledgements

We are grateful to study participants. We thank Alvaro Hernandez at the University of Illinois Roy J. Carver Biotechnology Center for outstanding DNA sequencing services. This research was supported by National Science Foundation Graduate Research Fellowship DGE-114747 (D.S.), National Institute of General Medical Sciences of the National Institutes of Health T32GM007276 (D.S.), Helmsley Foundation grant 2014PG-IBD014 (D.A.R.), Thomas C. and Joan M. Merigan Endowment at Stanford University (D.A.R.), and Chan Zuckerburg Biohub Microbiome Initiative (D.A.R.).

REFERENCES

1. Benchimol EI, Fortinsky KJ, Gozdyra P, et al. Epidemiology of pediatric inflammatory bowel disease: A systematic review of international trends. Inflamm Bowel Dis. 2011;17:423–39.

2. Lichtenstein GR, McGovern DPB. Using Markers in IBD to Predict Disease and Treatment Outcomes: Rationale and a Review of Current Status. Am J Gastroenterol (Supplement). 2016;3:17–26.

3. Soubières AA. Emerging role of novel biomarkers in the diagnosis of inflammatory bowel disease. World J Gastrointest Pharmacol Ther. 2016;7:41–50.

4. Khor B, Gardet A, Xavier RJ. Genetics and pathogenesis of inflammatory bowel disease. Nature 2011;474:307–317.

5. Papa E, Docktor M, Smillie C, et al. Non-invasive mapping of the gastrointestinal microbiota identifies children with inflammatory bowel disease. PLoS ONE. 2012;7:e39242–12.

6. Shaw KA, Bertha M, Hofmekler T, et al. Dysbiosis, inflammation, and response to treatment: a longitudinal study of pediatric subjects with newly diagnosed inflammatory bowel disease. Genome Med. 2016;8:75.

7. Gevers D, Kugathasan S, Denson LA, et al. The Treatment-Naive Microbiome in New-Onset Crohn's Disease. Cell Host Microbe. 2014;15:382–392.

8. Manichanh C, Rigottier-Gois L, Bonnaud E, et al. Reduced diversity of faecal microbiota in Crohn's disease revealed by a metagenomic approach. Gut. 2006;55:205–211.

9. Dethlefsen L, Huse S, Sogin ML, et al. The Pervasive Effects of an Antibiotic on the Human Gut Microbiota, as Revealed by Deep 16S rRNA Sequencing. PLoS Biol. 2008;6:e280.

10. Scribano ML. Use of antibiotics in the treatment of Crohn's disease. World J Gastroenterol. 2013;19:648–6.

11. Levine A, Kori M, Kierkus J, et al. Azithromycin and metronidazole versus metronidazole-based therapy for the induction of remission in mild to moderate paediatric Crohn's disease: a randomised controlled trial. Gut. 2018;gutjnl–2017–315199–10.

12. Levine A, Turner D. Combined azithromycin and metronidazole therapy is effective in inducing remission in pediatric Crohn's disease. J Crohns Colitis. 2011;5:222–226.

13. Caporaso JG, Kuczynski J, Stombaugh J, et al. QIIME allows analysis of high-throughput community sequencing data. Nat Meth. 2010;7:335–336.

14. Callahan BJ, McMurdie PJ, Rosen MJ, et al. DADA2: High-resolution sample inference from Illumina amplicon data. Nat Meth. 2016;13:581–583.

15. McMurdie PJ, Holmes S. phyloseq: an R package for reproducible interactive analysis and graphics of microbiome census data. PLoS ONE 2013;8:e61217.

16. Dethlefsen L, Relman DA. Incomplete recovery and individualized responses of the human distal gut microbiota to repeated antibiotic perturbation. Proc Natl Acad Sci USA. 2011;108 Suppl:4554–4561.

17. Lozupone C, Knight R. UniFrac: a new phylogenetic method for comparing microbial communities. Appl Environ Microbiol. 2005;71:8228–8235.

18. Retsema JA, Girard AE, Girard D, et al. Relationship of high tissue concentrations of azithromycin to bactericidal activity and efficacy in vivo. J Antimicrob Chemother. 1990;25 Suppl A:83–89.

19. Pascal V, Pozuelo M, Borruel N, et al. A microbial signature for Crohn's disease. Gut. 2017;66:813–822.

20. Sullivan A, Edlund C, Nord CE. Effect of antimicrobial agents on the ecological balance of human microflora. Lancet Infect Dis. 2001;1:101–114.

21. Weber D, Hiergeist A, Weber M, et al. Detrimental effect of broad-spectrum antibiotics on intestinal microbiome diversity in patients after allogeneic stem cell transplantation: Lack of commensal sparing antibiotics. Clin Infect Dis. 2018; doi: 10.1093/cid/ciy711.

22. Wlodarska M, Willing B, Keeney KM, et al. Antibiotic Treatment Alters the Colonic Mucus Layer and Predisposes the Host to Exacerbated *Citrobacter rodentium*-Induced Colitis. Infect Immun. 2011;79:1536–1545.

23. Høiby N, Bjarnsholt T, Givskov M, et al. Antibiotic resistance of bacterial biofilms. Int J Antimicrob Agents. 2010;35:322–332.

24. Lutz L, Pereira DC, Paiva RM, et al. Macrolides decrease the minimal inhibitory concentration of anti-pseudomonal agents against *Pseudomonas aeruginosa* from cystic fibrosis patients in biofilm. BMC Microbiol. 2012;12:196.

25. Glasser AL, Boudeau J, Barnich N, et al. Adherent invasive *Escherichia coli* strains from patients with Crohn's disease survive and replicate within macrophages without inducing host cell death. Infect Immun. 2001;69:5529–5537.

26. Martinez-Medina M, Naves P, Blanco J, et al. Biofilm formation as a novel phenotypic feature of adherent-invasive *Escherichia coli* (AIEC). BMC Microbiol. 2009;9:202–16.

27. Darfeuille-Michaud A, Boudeau J, Bulois P, et al. High prevalence of adherent-invasive *Escherichia coli* associated with ileal mucosa in Crohn's disease. Gastroenterology. 2004;127:412–421.

28. Miller WR, Munita JM, Arias CA. Mechanisms of antibiotic resistance in enterococci. Expert Rev Anti Infect Ther. 2014;12:1221–1236.

29. Lebreton F, van Schaik W, Manson McGuire A, et al. Emergence of Epidemic Multidrug-Resistant Enterococcus faecium from Animal and Commensal Strains. MBio. 2013;4:1–10.

30. Ghosh S, van Heel D, Playford RJ. Probiotics in inflammatory bowel disease: is it all gut flora modulation? Gut. 2004;53:620–622.

31. Dieleman LA, Goerres MS, Arends A, et al. Lactobacillus GG prevents recurrence of colitis in HLA-B27 transgenic rats after antibiotic treatment. Gut. 2003;52:370–376.

32. Borruel N, Carol M, Casellas F, et al. Increased mucosal tumour necrosis factor alpha production in Crohn's disease can be downregulated *ex vivo* by probiotic bacteria. Gut. 2002;51:659–664.

33. Prantera C, Scribano ML, Falasco G, et al. Ineffectiveness of probiotics in preventing recurrence after curative resection for Crohn's disease: a randomised controlled trial with Lactobacillus GG. Gut. 2002;51:405–409.

34. Marteau P, Lémann M, Seksik P, et al. Ineffectiveness of *Lactobacillus johnsonii* LA1 for prophylaxis of postoperative recurrence in Crohn's disease: a randomised, double blind, placebo controlled GETAID trial. Gut. 2006;55:842–847.

FIGURE LEGENDS

Fig. 1. Study design and clinical outcomes. **a** At week 0, 67 pediatric Crohn's Disease patients were randomly assigned to one of two treatment groups: MET subjects received 20 mg/kg metronidazole twice daily (maximum of 1000 mg/day) for 8 weeks, while MET+AZ subjects received metronidazole plus 7.5 mg/kg azithromycin (maximum of 500 mg/day) once a day for 5 consecutive days, followed by a 2-day drug holiday, each week for the first 4 weeks and then stepped down to 3 consecutive days of the same dose with a 4-day drug holiday, per week over the subsequent 4 weeks. Metronidazole (MET, red, n = 36) or metronidazole and azithromycin (MET+AZ, blue, n = 31). Patients not in remission between weeks 4 and 8 could be offered open-label azithromycin based on physician assessment (MET/MET+AZ, purple, n = 11), and are displayed as a distinct patient cohort from weeks 4 to 12. Stool samples were collected at weeks 0, 4, 8, and 12 (vertical gold bars). **b** Pediatric Crohn's Disease Activity Index (PCDAI) for subjects at weeks 0, 4, 8, and 12. Treatment groups (MET, red; MET+AZ, blue; MET/MET+AZ, purple) are in columns, while the rows are groups of subjects that were either in remission (top) or not in remission (bottom) at week 4.

Fig. 2. Microbiota response to antibiotic therapy. **a** Alpha diversity measured by Faith's Phylogenetic Diversity, segregated by treatment group (MET, red; MET+AZ, blue; MET/MET+AZ, purple) and week. Treatment group colors are darker during antibiotic treatment. *p*-values are displayed for between-treatment comparisons (Wilcoxon Test). **b** Boxplot of the median intra-subject unweighted UniFrac distance between samples collected during consecutive time points. **c-e** Principal coordinates analysis (PCoA) on the unweighted UniFrac distance for all samples and all subjects. Samples are colored by **c** current antibiotic use, yes/no; **d** current antibiotic use and treatment group; or **e** current disease state, in remission or not.

Fig. 3. Microbial abundances shift in response to antibiotic exposure. Heat map of microbial abundances partitioned by treatment group and week. Amplicon sequence variant (ASV) abundances were $\log_{10}$-transformed prior to plotting. The displayed ASVs were present in ≥ 20% of samples and had statistically significant shifts in abundance between weeks 0 and 4 in either the MET or MET+AZ treatment groups, as denoted by the colors on the y-axis.

Fig. 4. Microbiota at time of remission reflects antibiotic exposure. **a** Beta-diversity measured by Bray-Curtis dissimilarity between samples in remission and non-remission among MET and MET+AZ subjects during antibiotic treatment (weeks 4 and 8). **b** PCoA on the Bray-Curtis dissimilarity of stool samples collected during antibiotic treatment (weeks 4 and 8). Remission samples (PERMANOVA, p = 0.0009), no remission samples (PERMANOVA, p = 0.1848). Significance of treatment group clustering was determined by PERMANOVA (`adonis`) with 1,000 permutations.

Fig 5. Random Forest models classify disease remission from microbiota profiles. **a** The ROC curves indicate the accuracy of the random forest classification models built using microbiota data. Color of lines indicates the dataset on which the model was trained (Model 1, MET weeks 4 and 8, red; Model 2, MET weeks 0, 4 and 8, blue). Solid lines indicate accuracy of the model in classifying remission in patients from the same treatment group (MET), while the dashed lines indicate the accuracy of each model for classifying remission in patients from the MET+AZ treatment group. *AUC* Area under the curve. **b** Variable importance values for the 10 most important ASVs used to build each random forest model are plotted against each other. Points are labeled by ASV number. Point color indicates the importance score (Model 1 specific, red;

Model 2 specific, blue; both models, gray). **c** Log-transformed abundances of top 20 ASVs that were of common importance for both Random Forest models.

Supplemental Figure 1. Pre-treatment microbiota structure predicts treatment outcome. **a** The alpha-diversity of samples collected at baseline (week 0) grouped by their treatment group and remission status at week 4 (Wilcoxon Test). **b** The gray ROC curve indicates the accuracy of the random forest classification model built using microbiome data from week 0 as well as gender, age, disease duration, Paris classification, pre-antibiotic immunomodulators, PCDAI and CRP to predict response to treatment at week 4. *AUC* Area under the curve. **c** Abundances of ASV clusters that are important for the remission-forecasting random forest models. Abundances were transformed using a variance stabilizing transformation (Bioconductor package `vsn`).

Table 1. Subject Demographics.

Treatment Group	# Samples	# Subjects	Female/Male	Mean Age (years) ± SD	Mean Disease Duration (years) ± SD	Baseline PCDAI ± SD
MET	120	36	20/16	13.5 ± 3.1	0.7 ± 1	19.6 ± 8.1
MET+AZ	112	31	6/25	14.2 ± 3.1	1.1. ± 1.1	22 ± 9

67 pediatric Crohn's Disease patients were randomly assigned to treatment with either metronidazole (MET) or metronidazole plus azithromycin (MET+AZ). Only sex differed significantly between the two groups ($P < 0.01$). *PCDAI* pediatric Crohn's Disease activity index. *SD* standard deviation.

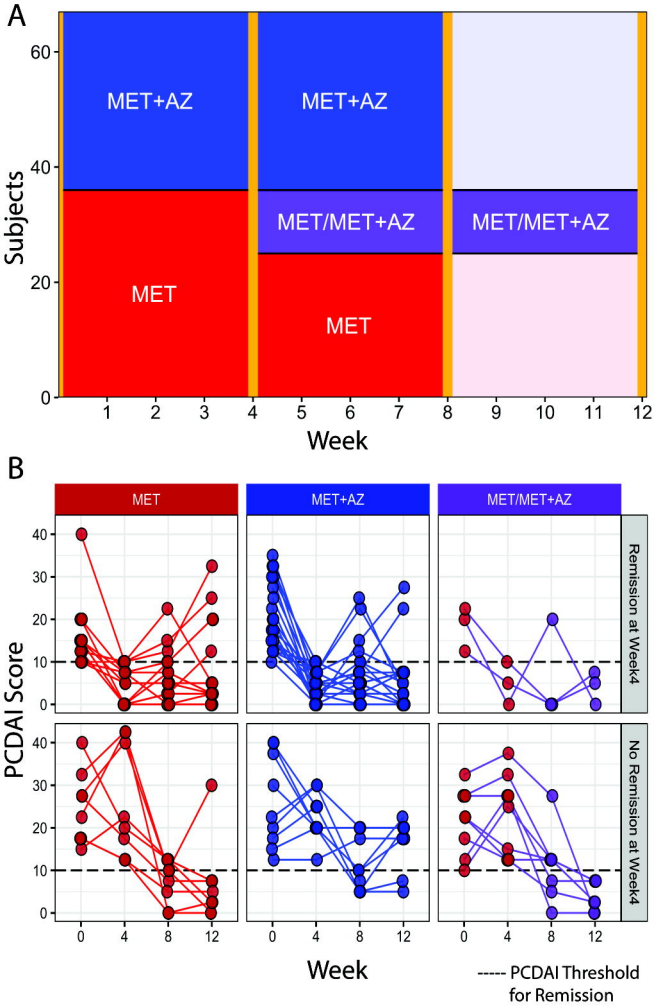
A
Subjects
Week
MET+AZ
MET+AZ
MET/MET+AZ
MET/MET+AZ
MET
MET
B
MET
MET+AZ
MET/MET+AZ
Remission at Week4
No Remission at Week4
PCDAI Score
Week
----- PCDAI Threshold for Remission

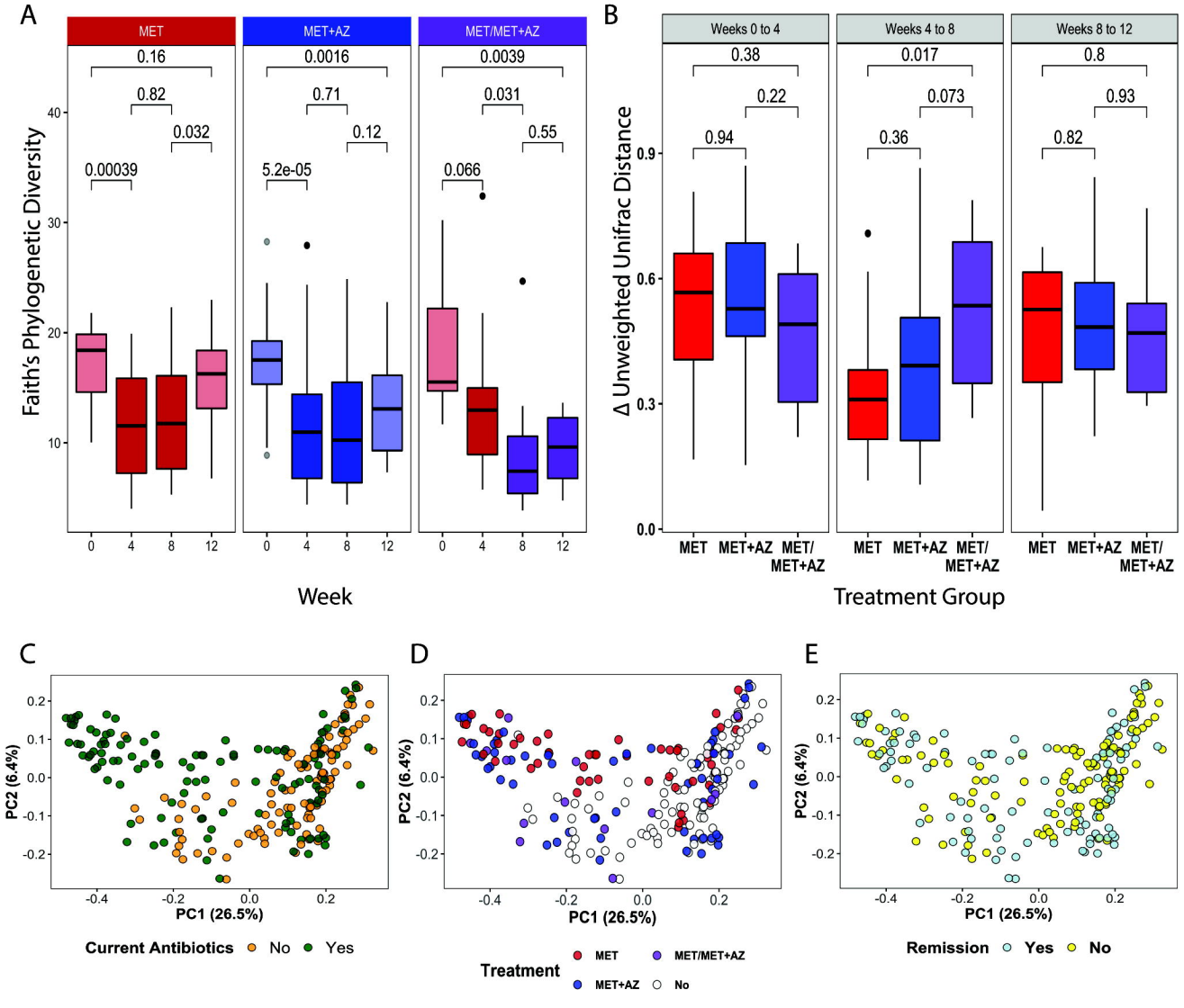
A
MET
MET+AZ
MET/MET+AZ
0.16
0.82
0.032
0.00039
0.0016
0.71
0.12
5.2e-05
0.0039
0.031
0.55
0.066
Faith's Phylogenetic Diversity
Week
B
Weeks 0 to 4
Weeks 4 to 8
Weeks 8 to 12
0.38
0.22
0.94
0.017
0.073
0.36
0.8
0.93
0.82
Δ Unweighted Unifrac Distance
MET
MET+AZ
MET/ MET+AZ
Treatment Group
C
PC1 (26.5%)
PC2 (6.4%)
Current Antibiotics
No
Yes
D
Treatment
MET
MET+AZ
MET/MET+AZ
No
E
Remission
Yes
No

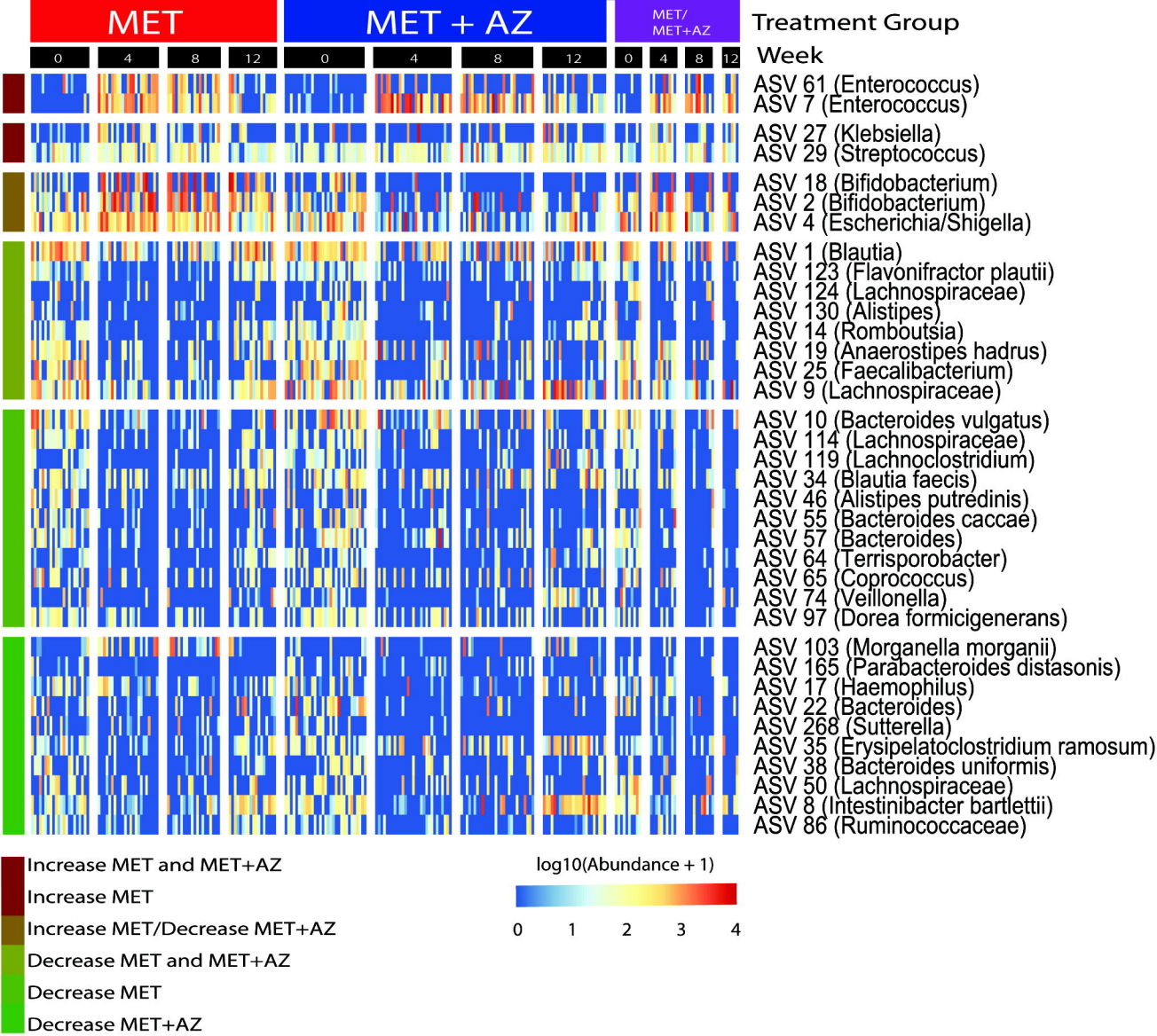
MET
MET + AZ
MET/
MET+AZ
Treatment Group
0
4
8
12
Week
ASV 61 (Enterococcus)
ASV 7 (Enterococcus)
ASV 27 (Klebsiella)
ASV 29 (Streptococcus)
ASV 18 (Bifidobacterium)
ASV 2 (Bifidobacterium)
ASV 4 (Escherichia/Shigella)
ASV 1 (Blautia)
ASV 123 (Flavonifractor plautii)
ASV 124 (Lachnospiraceae)
ASV 130 (Alistipes)
ASV 14 (Romboutsia)
ASV 19 (Anaerostipes hadrus)
ASV 25 (Faecalibacterium)
ASV 9 (Lachnospiraceae)
ASV 10 (Bacteroides vulgatus)
ASV 114 (Lachnospiraceae)
ASV 119 (Lachnoclostridium)
ASV 34 (Blautia faecis)
ASV 46 (Alistipes putredinis)
ASV 55 (Bacteroides caccae)
ASV 57 (Bacteroides)
ASV 64 (Terrisporobacter)
ASV 65 (Coprococcus)
ASV 74 (Veillonella)
ASV 97 (Dorea formicigenerans)
ASV 103 (Morganella morganii)
ASV 165 (Parabacteroides distasonis)
ASV 17 (Haemophilus)
ASV 22 (Bacteroides)
ASV 268 (Sutterella)
ASV 35 (Erysipelatoclostridium ramosum)
ASV 38 (Bacteroides uniformis)
ASV 50 (Lachnospiraceae)
ASV 8 (Intestinibacter bartlettii)
ASV 86 (Ruminococcaceae)
Increase MET and MET+AZ
Increase MET
Increase MET/Decrease MET+AZ
Decrease MET and MET+AZ
Decrease MET
Decrease MET+AZ
log10(Abundance + 1)
0
1
2
3
4

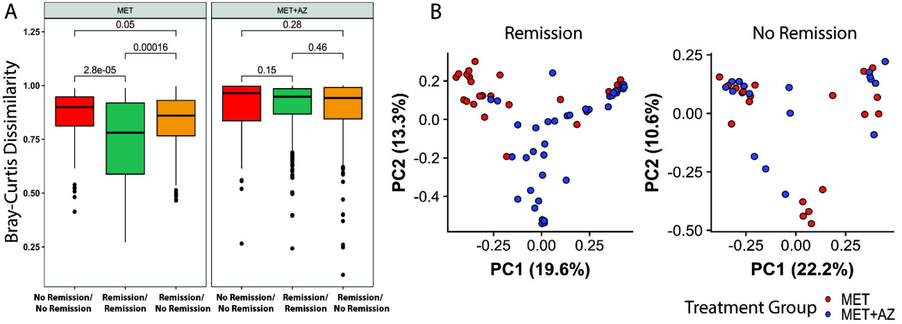
A
MET
MET+AZ
0.05
0.00016
2.8e-05
0.28
0.46
0.15
Bray-Curtis Dissimilarity
1.25
1.00
0.75
0.50
0.25
No Remission/ No Remission
Remission/ Remission
Remission/ No Remission
No Remission/ No Remission
Remission/ Remission
Remission/ No Remission

B
Remission
No Remission
PC2 (13.3%)
PC1 (19.6%)
PC2 (10.6%)
PC1 (22.2%)
0.2
0.0
-0.2
-0.4
0.25
0.00
-0.25
-0.50
-0.25
0.00
0.25
Treatment Group
MET
MET+AZ

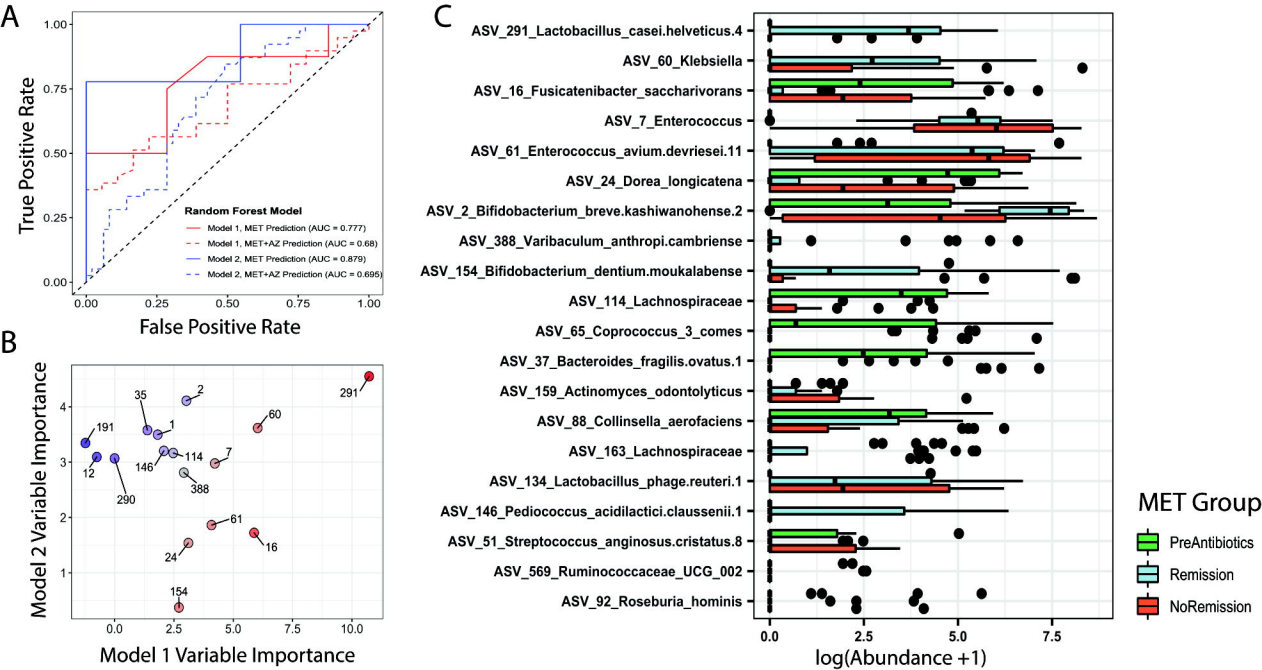
A
True Positive Rate
False Positive Rate
Random Forest Model
Model 1, MET Prediction (AUC = 0.777)
Model 1, MET+AZ Prediction (AUC = 0.68)
Model 2, MET Prediction (AUC = 0.879)
Model 2, MET+AZ Prediction (AUC = 0.695)
B
Model 2 Variable Importance
Model 1 Variable Importance
C
ASV_291_Lactobacillus_casei.helveticus.4
ASV_60_Klebsiella
ASV_16_Fusicatenibacter_saccharivorans
ASV_7_Enterococcus
ASV_61_Enterococcus_avium.devriesei.11
ASV_24_Dorea_longicatena
ASV_2_Bifidobacterium_breve.kashiwanohense.2
ASV_388_Varibaculum_anthropi.cambriense
ASV_154_Bifidobacterium_dentium.moukalabense
ASV_114_Lachnospiraceae
ASV_65_Coprococcus_3_comes
ASV_37_Bacteroides_fragilis.ovatus.1
ASV_159_Actinomyces_odontolyticus
ASV_88_Collinsella_aerofaciens
ASV_163_Lachnospiraceae
ASV_134_Lactobacillus_phage.reuteri.1
ASV_146_Pediococcus_acidilactici.claussenii.1
ASV_51_Streptococcus_anginosus.cristatus.8
ASV_569_Ruminococcaceae_UCG_002
ASV_92_Roseburia_hominis
log(Abundance +1)
MET Group
PreAntibiotics
Remission
NoRemission